tvst

Cornea & External Disease

Effect of Recombinant Human Lubricin on Model Tear Film Stability

Kiara W. Cui[1], Vincent X. Xia[1], Daniel Cirera-Salinas[2], David Myung[1,3], and Gerald G. Fuller[1]

[1] Stanford Department of Chemical Engineering, Stanford, CA, USA
[2] Global Drug Development, Novartis Pharma, Basel, Switzerland
[3] Byers Eye Institute at the Stanford School of Medicine, Stanford, CA, USA

Correspondence: Gerald G. Fuller, Stanford Department of Chemical Engineering, 443 Via Ortega, Room 086, Stanford, CA 94305, USA.
e-mail: ggf@stanford.edu

Received: March 28, 2022
Accepted: August 15, 2022
Published: September 16, 2022

Keywords: tear film; dry eye; fluid film stability; adsorption; image quantification; *rh*-lubricin; tear film break-up

Citation: Cui KW, Xia VX, Cirera-Salinas D, Myung D, Fuller GG. Effect of recombinant human lubricin on model tear film stability. Transl Vis Sci Technol. 2022;11(9):9, https://doi.org/10.1167/tvst.11.9.9

Purpose: To investigate and quantify the effect of recombinant human lubricin (*rh*-lubricin) on model tear film stability.

Methods: A custom-built, interferometry-based instrument called the Interfacial Dewetting and Drainage Optical Platform was used to create and record the spatiotemporal evolution of model acellular tear films. Image segmentation and analysis was performed in MATLAB to extract the most essential features from the wet area fraction versus time curve, namely the evaporative break-up time and the final wet area fraction (A10). These two parameters indicate the tear film stability in the presence of *rh*-lubricin in its unstressed and stressed forms.

Results: Our parameters successfully captured the trend of increasing tear film stability with increasing *rh*-lubricin concentration, and captured differences in *rh*-lubricin efficacy after various industrially relevant stresses. Specifically, aggregation and fragmentation caused by a 4-week, high temperature stress condition negatively impacted *rh*-lubricin's ability to maintain model tear film stability. Adsorbed *rh*-lubricin alone was not sufficient to resist break-up and maintain full area coverage of the model tear film surface.

Conclusions: Our results demonstrate that fragmentation and aggregation can negatively impact *rh*-lubricin's ability to maintain a stable tear film. In addition, the ability of *rh*-lubricin to maintain wetted area coverage is due to both freely dispersed and adsorbed *rh*-lubricin.

Translational Relevance: Our platform and analysis method provide a facile, intuitive, and clinically relevant means to quantify the effect of ophthalmic drugs and formulations intended for improving tear film stability, as well as capture differences between variants related to drug stability and efficacy.

Introduction

A several micron-thick, multilayer structure called the tear film is crucial to the function and comfort of our ocular surface (Fig. 1A). Within the tear film, membrane-bound and secreted glycoproteins called mucins serve important roles, such as lubrication between corneal and conjunctival cells when blinking, maintaining the hydration through gel formation, and serving as a barrier against external pathogens.[1,2] Structurally, mucins are composed of a serine- and threonine-rich protein backbone and a high degree of O-linked oligosaccharide glycosylation, which makes up the majority of the molecule's weight.[1] It is thought that this structure is key to protection of the ocular surface. Altered expression of mucins within the tear film is one of the causes of dry eye disease (DED), an ocular pathology that affects hundreds of millions of patients worldwide. According to the most recent definition, DED is characterized by discomfort, blurred vision, tear film instability, hyperosmolarity, inflammation, neurosensory abnormalities, and even ocular surface damage.[1,3,4] Although this is such

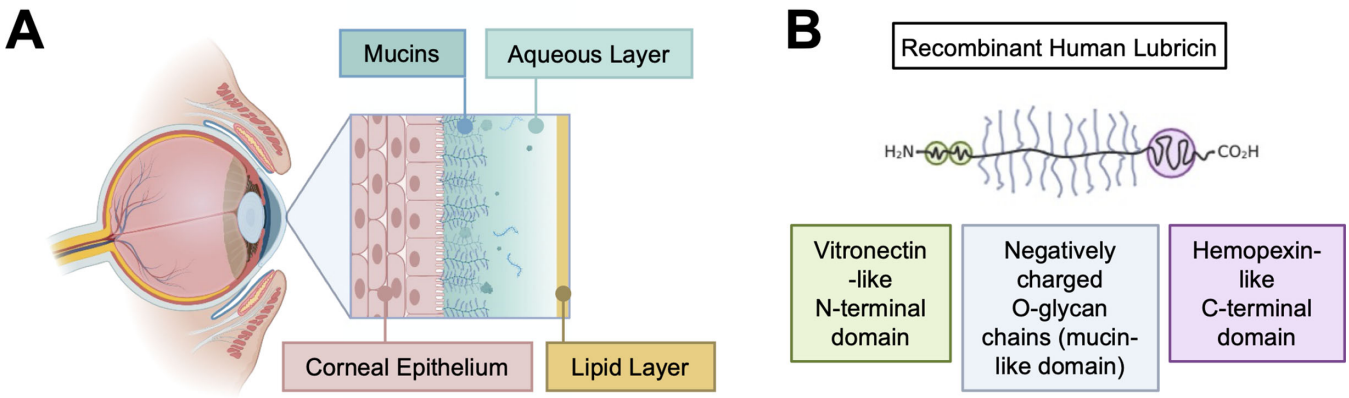

Figure 1. Use of recombinant human lubricin (*rh*-lubricin) to address symptoms of DED associated with a mucin-deficient tear film. (**A**) Structure of the human tear film, which consists of an aqueous layer with increasing concentrations of mucins and an outermost lipid layer to assist in tear film stability. Mucins serve lubrication, hydration, and barrier functions within the tear film. Mucin deficiency in the tear film can lead to discomfort and can ultimately contribute to DED symptoms.[1,3] (**B**) The mucin-like glycoprotein *rh*-lubricin is a candidate in addressing DED symptoms; representative structure is shown.

a widespread condition, few effective treatments exist despite extensive research and testing owing to the multifaceted nature of the disease and complexity of the tear film.[5]

One molecule that has shown promise, however, is recombinant human lubricin (*rh*-lubricin), a mucin-like glycoprotein expressed by ocular surface epithelia as a product of the proteoglycan 4 (PRG4) gene.[6] Lubricin has been shown to significantly reduce shear stress and friction during blink cycles[6–8] and demonstrated a significant improvement in DED symptoms in a randomized clinical trial when compared with sodium hyaluronate eye drops.[9] The structure of *rh*-lubricin is shown in Figure 1B. It is composed of a central bottlebrush mucin-like domain made of negatively charged O-glycan chains and vitronectin-like and hemopexin-like adhesive domains at its N-terminal and C-terminal domains, respectively.[10]

To understand the potential role of *rh*-lubricin in tear film stability, previous work has investigated the ability of *rh*-lubricin to stabilize thin liquid films on a curved, hydrophilic glass substrate that mimics the ocular surface.[11] Remarkably, these model tear films remained stable for minutes to hours in the presence of *rh*-lubricin. This stability phenomenon was hypothesized to be driven by a combination of evaporation-driven solutocapillary flows, a stabilizing disjoining pressure, and a hydrated, adsorbed *rh*-lubricin layer on the glass dome. *rh*-Lubricin was also better able to maintain thin film stability at an equivalent concentration when compared with another commercially available glycoprotein, bovine submaxillary mucin.

In this work, we designed two metrics to quantify and thus further our understanding of how *rh*-lubricin is able to stabilize model tear films. Specifically, we condensed the rich spatiotemporal information present in the wetted area fraction evolution plot to extract (i) the evaporative break-up time (EBUT), which represents how quickly the onset of evaporation-driven film instability occurs, and (ii) the final wetted area fraction (A10), which represents the thin film's ability to keep the model ocular surface hydrated over time. Our data corroborate previously published trends showing that higher *rh*-lubricin concentrations are better able to stabilize the tear film against evaporation and break-up. We then compared the efficacy of unstressed *rh*-lubricin samples with that of *rh*-lubricin samples exposed to forced degradation from a variety of industrially relevant stresses. We were able to capture differences in model tear film stability using the EBUT and A10 parameters described elsewhere in this article. Finally, we performed a mechanistic study to understand the role of adsorbed and freely dispersed *rh*-lubricin in model tear film stabilization. By providing a facile way to quantify and compare the effect of *rh*-lubricin on thin film stability, we hope that these metrics will ultimately help to elucidate the physical mechanisms by which *rh*-lubricin protects the ocular surface.

Methods

rh-Lubricin Sample Preparation

rh-Lubricin (Novartis Pharma AG, Basel, Switzerland) was provided in a stock solution at a concentration of 2.0 mg/mL in a saline buffer at neutral

Table. Summary of All *rh*-Lubricin Samples Used in This Study.

Sample Name	Condition
Drug substance (DS)	Unstressed *rh*-lubricin stored at pH 7.0, 25°C, 4 weeks, control for temperature and pH stresses
Temperature stressed (TS)	pH 7.0, 40°C, 75% relative humidity, 4 weeks
pH stressed (pHS)	pH 9.0, 25°C, 2 weeks
Control A	Unstressed *rh*-lubricin stored at 25°C, control for freeze–thaw stresses
Freeze–thaw (F/T)	10 cycles of freezing at −20°C and thawing at 25°C
Control B	Unstressed *rh*-lubricin stored at 25°C for 5 days, control for shaking stress
Shaking (Sh)	Shaken at 150 rpm using reciprocating movement at ambient temperature for 5 days
Control C	DS containing methionine and incubated 8 hours at 25°C, control for oxidative stress
Oxidation t = 0	Incubated at 25°C and 500:1 H_2O_2 to protein molar ratio, quenched immediately by methionine
Oxidation t = 8 hours	Incubated at 25°C and 500:1 H_2O_2 to protein molar ratio, quenched after 8 hours by methionine
Light (1×, plastic)	Exposure to 1-fold of the light standard (visible and UV) following guideline Q1B of the International Conference on Harmonization while stored in plastic
Light (1×, glass)	Exposure to 1-fold of the light standard following guideline Q1B of the International Conference on Harmonization while stored in glass
Light (5×, glass)	Exposure to 5-fold of the light standard following guideline Q1B of the International Conference on Harmonization while stored in plastic

pH with 0.02 w/v% polysorbate 20 (PS20). A delivery vehicle solution containing the buffer and PS20, but without *rh*-lubricin, was also provided. To investigate the effect of forced degradation on the efficacy of the molecule, *rh*-lubricin stock solutions were subjected to various stresses chosen based on regulatory guidelines. All samples were derived from the same batch of *rh*-lubricin, and details of all conditions are shown in Table.

Stock samples were stored at −80°C until the day of the experiment, at which point they were rapidly thawed in a 37°C water bath. Solutions were prepared by diluting the stock in 1× phosphate-buffered saline (PBS; Corning, Corning, NY) at a pH of 7.4 with final *rh*-lubricin concentrations of 50, 5, 2.5, 1.25, 0.5, 0.25, 0.125, and 0.05 µg/mL. An equivalent volume fraction of stock solution in PBS was used for the vehicle control experiments, and pure 1× PBS was used for PBS control experiments.

i-DDrOP Experiments

A custom-built, interferometry-based platform called the Interfacial Dewetting and Drainage Optical Platform (i-DDrOP) was used to conduct model tear film stability experiments, and a full description of the instrument and experimental methods can be found in previous literature.[11–17] In addition to the setup previously described, an acrylic enclosure with mesh top was built around the instrument to decrease the effect of ambient air flow (Fig. 2A).

Briefly, a UV-fused silica (hydrophilic glass) plano-convex dome, with a radius of curvature mimicking that of the human eye, was placed atop a motorized stage that runs upward through a Teflon Langmuir trough. After rinsing with ethanol, acetone, and Milli-Q water, the trough was filled with 20 mL of the prepared lubricin or control solution, and the dome is submerged 1 mm below the air–liquid interface. The solution was heated to a physiological temperature of 37°C for 15 minutes, during which *rh*-lubricin is also able to adsorb to the surface of the glass dome. Then, the stage raised the dome 1 mm above the air–liquid interface at a speed of 1.0 mm/s, capturing a thin liquid film, which serves as the model tear film. The interference patterns within this film generated by an overhead diffuse light source were captured by a CCD camera for a duration of 10 minutes. The ambient relative humidity was recorded for each experimental session and typically ranged from 30% to 40%.

Before each experiment, domes were cleaned in a solution of 2% Hellmanex III (Hellma Analytics, Plainview, NY) in Milli-Q water in glass vials on a rotating shaker for at least 15 minutes and up to overnight.

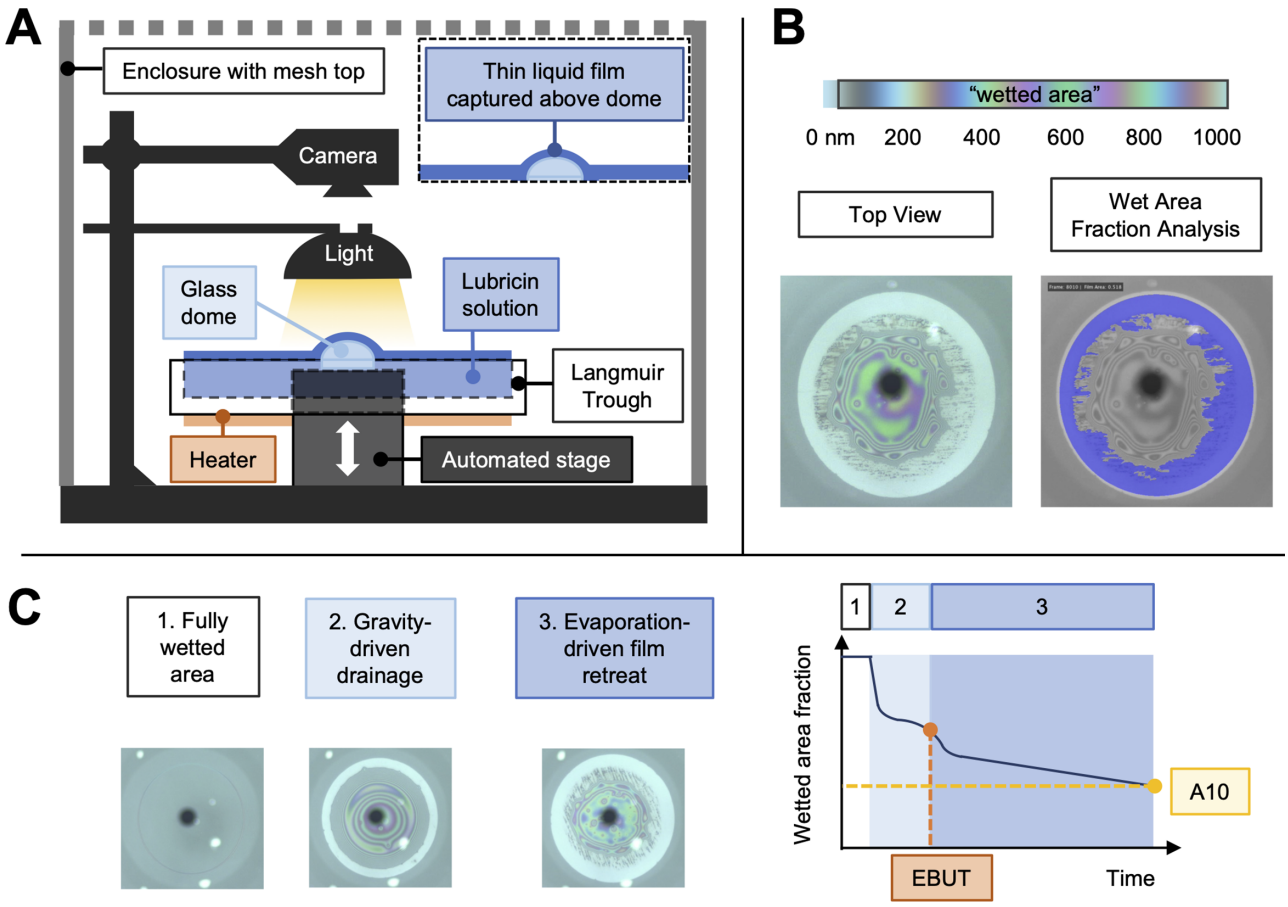

Figure 2. The i-DDrOP was used to perform studies of model tear film stability in the presence of *rh*-lubricin. (**A**) Simplified schematic showing the platform, in which a thin liquid film mimicking the tear film can be captured on a glass dome atop a motorized stage. (**B**) Interference patterns seen from a top view of the model tear film can be mapped back to film thickness, as shown in the color map. Areas in which film thickness is above approximately 50 nm are considered "wetted." The wetted area fraction is quantified using a segmentation algorithm built in MATLAB. (**C**) Up to three regimes of film evolution are typically observed for thin aqueous films containing *rh*-lubricin. From the wetted area fraction versus time plots, two parameters of interest can be extracted. The EBUT represents the time at which evaporation-driven film retreat begins, while the wetted area fraction at 10 minutes (A10) represents the fraction of the dome that remains wet (thickness of >50 nm) after being exposed to air for 10 minutes. The higher the EBUT and A10, the more stable the model tear film.

Domes were then gently wiped using lens cleaning tissues (ThorLabs, Newton, NJ) dotted with ethanol, acetone, and Milli-Q water, respectively. To ensure that the surface of the dome was clean and thus would not introduce dewetting artifacts, a dewetting experiment was conducted on the i-DDrOP using Milli-Q water to ensure linear, nonspontaneous film break-up from evaporation alone.[11]

Mechanistic Studies

To understand the effect of adsorbed versus freely dispersed *rh*-lubricin on tear film stability, glass domes were incubated at 37°C while submerged in a 50 µg/mL solution of *rh*-lubricin for 15 minutes. This condition simulates the maximum amount of *rh*-lubricin adsorption to the glass dome present in any i-DDrOP experiment. Separately, 20-mL aliquots of the vehicle and PBS were also heated to 37°C for 15 minutes. The dome was then removed from the *rh*-lubricin solution and placed on the motorized stage of the i-DDrOP, and the vehicle or PBS was added to the trough while maintaining the 37°C temperature. A 10-minute experiment monitoring the drainage of the model tear film was performed.

To perform experiments at 100% relative humidity, a solvent trap was placed between the dome and the light source. The underside of the trap was wetted with a small amount of 2% Hellmanex III solution to keep the surface optically clear. For experiments suppressing thermocapillary flows, the solution was not heated, and measurements were performed at room temperature.

Data Analysis

To condense the rich spatiotemporal data set from each i-DDrOP experiment, a wetted area fraction versus time analysis using a custom MATLAB algorithm was first performed. For this analysis, we defined any film thickness of more than approximately 50 nm as wet, as defined by the leftmost color band (Fig. 2B and Supplementary Movie S1). Cutoffs for hue, saturation, and value space were found using a single video frame that depicted wetted and nonwetted areas in the MATLAB Color Thresholder app. The total area (wetted area fraction equal to 1) was defined by an elliptical selection of the first frame at which the appearance of the total exposed dome area stabilized. In addition to the automatic detection of wetted versus nonwetted areas, the algorithm automatically excluded the central camera shadow from the analysis. All code is available publicly on GitHub at the following link: https://github.com/xiavincent/iddrop.

Two parameters were further extracted from the area fraction versus time curve as a quantification of tear film stability. The wetted area fraction at t = 10 minutes (A10) was found through a linear fit of the data points from t = 400 to 600 seconds and its intersection at t = 600 seconds using the MATLAB Curve Fitting Tool. The EBUT was calculated as the inflection point for the final decline in wetted area fraction using the MATLAB Curve Fitting Tool or recorded as 600 seconds if no decline in wetted area fraction was observed following the initial gravity-driven drainage regime (Fig. 2C). Graphs in Figure 4 were made using Prism 9.

Results

i-DDrOP Experiments

First, we sought to understand the behavior of unstressed *rh*-lubricin (drug substance [DS]) in our system as well as how well our chosen parameters classified this behavior. For all of our model tear film experiments, up to three regimes were seen on the wetted area fraction versus time plots (Fig. 2C). During the first regime, after raising the dome above the air–liquid interface, the film decreases in thickness but remains fully wetted, giving a constant wetted area fraction of 1. Next, the outer edges of the dome will experience gravity drainage owing to the higher film curvature in that region, as reflected in the first dip within the graph. Finally, a second dip may occur if the film continues to retreat owing to evaporation.

The final wetted area fraction parameter, A10, showed a gradual increase as a function of increasing concentration, with sample final frames shown in Figure 3A and corresponding representative videos shown in Supplementary Movie S2A. For the EBUT, we saw four main categories of model tear film behavior when varying the concentration (Fig. 3B, Supplementary Movie S2B). At the highest concentrations, the film re-expanded to fill the exposed area after gravity drainage, and this full recovery behavior was assigned an EBUT of 600 seconds because it remained fully stable over the 10-minute measurement period. In the metastable category, the area of the film remained constant after gravity drainage, and we again assigned this case an EBUT of 600 seconds owing to its stability. A slight decrease in concentration shifted the behavior into the two-stage break-up category, where all three regimes were seen in the wetted area fraction plot. In other words, film retreat owing to evaporation followed the gravity drainage stage, and this category exhibited an EBUT of 80 to 100 seconds. Finally, for the lowest concentrations of *rh*-lubricin as well as vehicle or PBS conditions, model tear film break-up exhibited a continuous decline between the gravity drainage and evaporative break-up regimes, giving an EBUT of 30 to 50 seconds. Overall, these studies showed that our analysis methods were sufficient for distinguishing variations in the ability of *rh*-lubricin to maintain model tear film stability, as a function of concentration.

All model tear films containing *rh*-lubricin exhibited oscillations in film thickness throughout the measurement period in the 300 to 600 nm range (Supplementary Movie S2A). This phenomenon was previously hypothesized to be driven by solutocapillary flows from the thinner, warmer, low surface tension region at the edges of the dome to the thicker, cooler, high surface tension region at the center of the dome.[11] We confirmed that these were the result of evaporation-driven Marangoni flows rather than thermocapillary flows; no oscillatory behavior was present when evaporation was suppressed, but oscillations were still observed when performing the experiment in the absence of a thermal gradient at room temperature (Supplementary Movie S3).

Forced Degradation Studies

To understand the effect of various modes of forced degradation on the ability of *rh*-lubricin to maintain model tear film stability, we conducted dose-dependence studies on each of the samples listed in Table. First, we investigated the effect of exposure to elevated temperature and pH (Fig. 4A, Supplementary

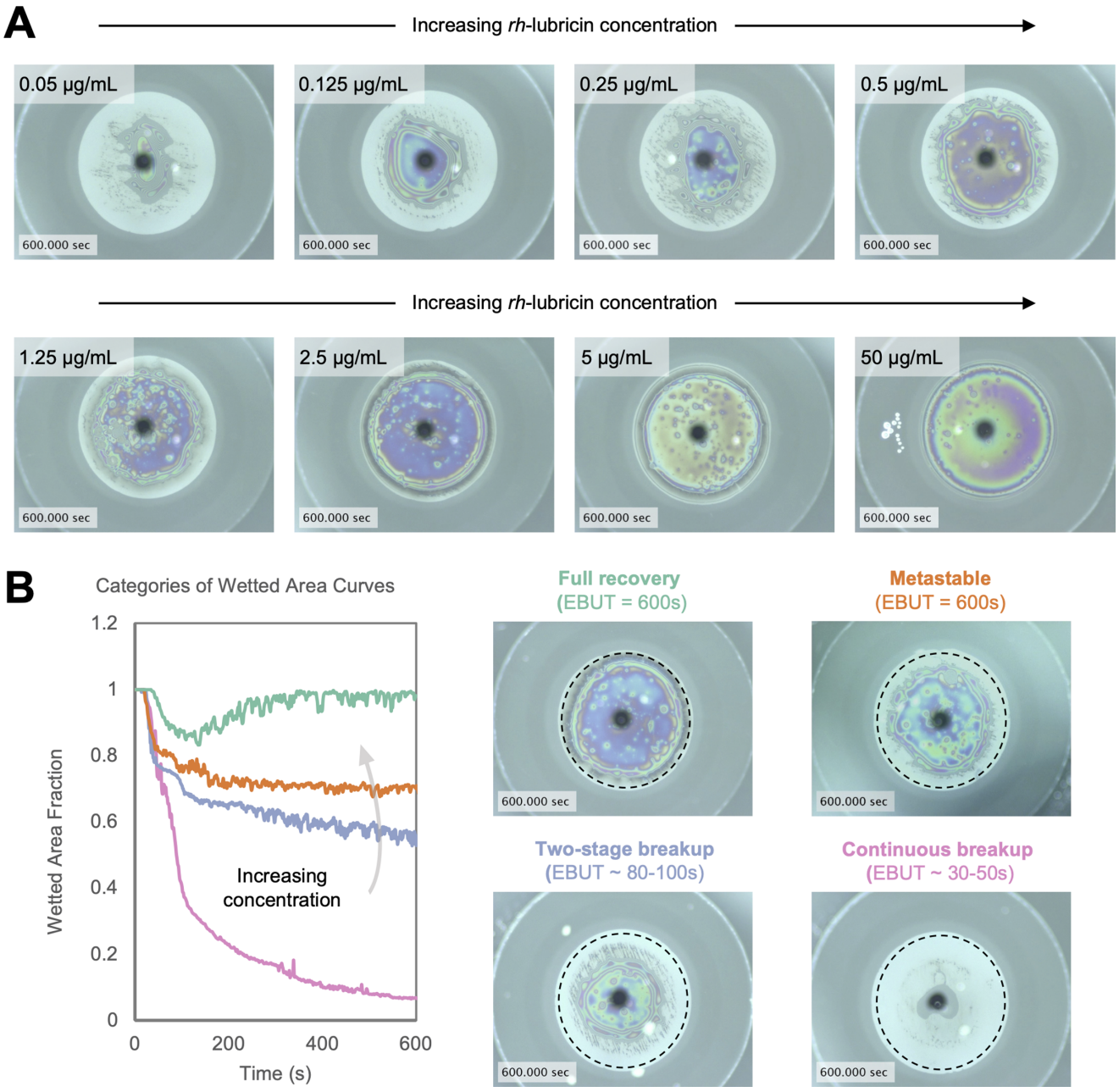

Figure 3. Both the EBUT and A10 parameters increased with increasing *rh*-lubricin concentration. (**A**) Representative snapshots of the wetted area fraction remaining at the end of the 10-minute measurement period. Remaining wet area coverage increases with increasing *rh*-lubricin concentration. (**B**) Four general categories of wetted area curves were observed with increasing *rh*-lubricin concentration; representative curves are shown on the left, with the black dotted line showing the analyzed area. Typical EBUT values for each category are shown to the right, where an EBUT of 600 seconds indicates that the model tear film remained fully stable (no onset of evaporative break-up) within the measurement period.

Fig. S1). Dynamic light scattering showed that the temperature-stressed *rh*-lubricin exhibited aggregation and fragmentation relative to the control (DS), whereas pH-stressed *rh*-lubricin exhibited high aggregation (Supplementary Fig. S2, Supplementary Table S1). For the temperature-stressed sample, both the EBUT and A10 versus concentration data reflected a decrease in efficacy for maintaining tear film stability, as indicated by a right-shifted dose–response curve. In contrast, the pH-stressed sample exhibited no significant difference when compared with the unstressed DS in either metric. The delivery vehicle condition showed a lower EBUT and A10 compared with DS at the equivalent concentration, suggesting that most

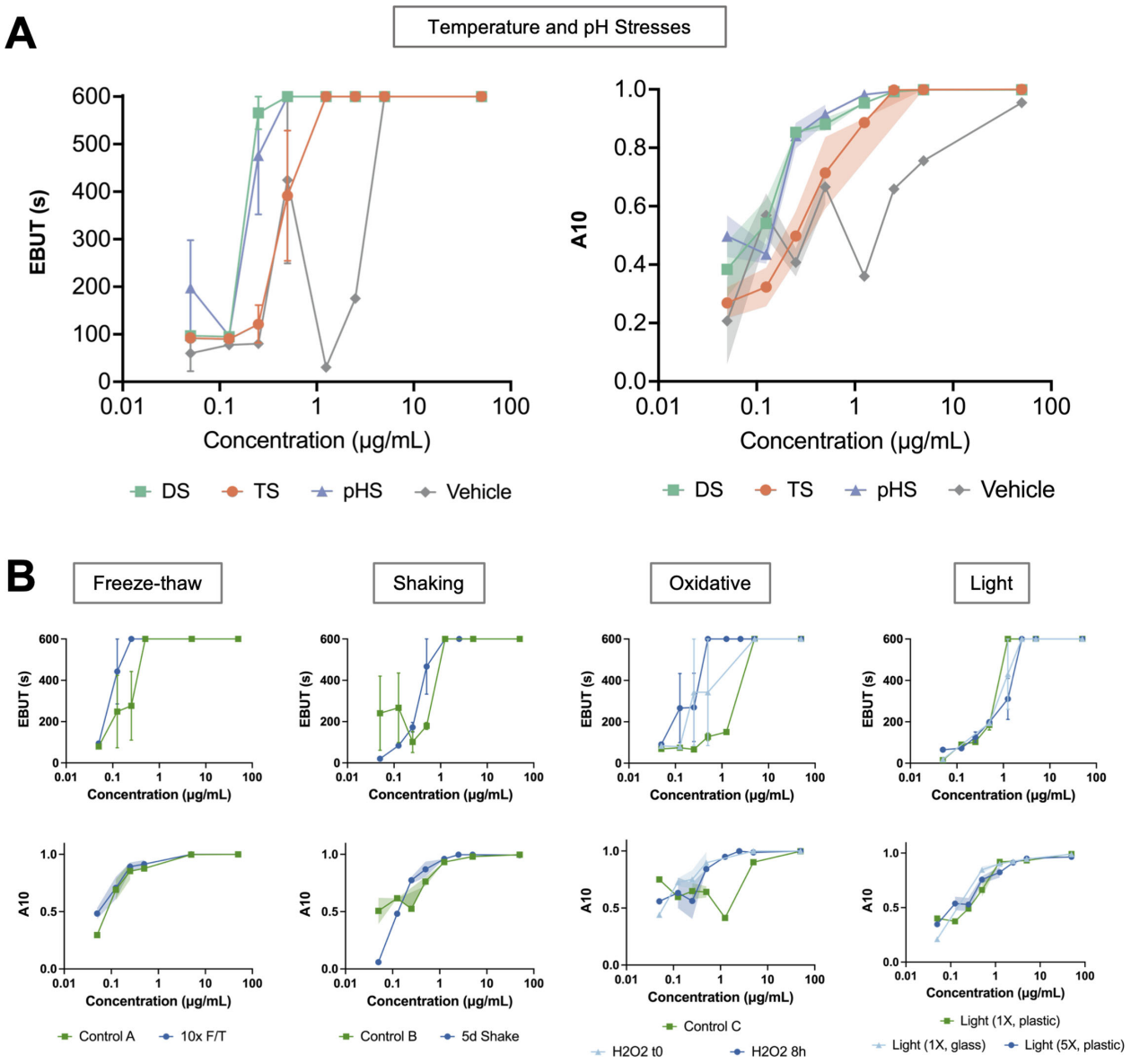

Figure 4. Prolonged elevated temperature stress had a detrimental effect on *rh*-lubricin's ability to maintain model tear film stability, while other forms of stress had a negligible effect. (**A**) Differences in EBUT and final wetted area fraction (A10) observed between unstressed DS, temperature-stressed (TS), and pH-stressed lubricin (pHS), and the vehicle. Note that an EBUT of 600 seconds indicates that film retreat is not seen during the 10-minute measurement period (data are mean ± standard error; $n = 1–8$) (also see Supplementary Fig. S1). (**B**) Differences in EBUT and A10 observed between unstressed *rh*-lubricin and samples subjected to freeze–thaw cycles, shaking, oxidative stresses, and light stresses (data are mean ± standard error; $n = 1–5$). Details for all conditions can be found in Table; see also Supplementary Figures S1, S2 and Supplementary Table S1.

of the effect on film stability can be attributed to *rh*-lubricin. The vehicle model tear films also displayed greater asymmetry and variability (Supplementary Movie S4). For additional forms of forced degradation, including freeze–thaw cycles, shaking, oxidative stress, and exposure to light, stressed *rh*-lubricin did not show a decrease in efficacy compared with controls (Fig. 4B).

Role of Adsorbed versus Freely Dispersed Lubricin

During the incubation and heating period before our measurements, *rh*-lubricin is able to adsorb to the hydrophilic glass dome surface.[11] To understand the relative roles of adsorbed *rh*-lubricin and freely dispersed *rh*-lubricin within the thin film, we performed

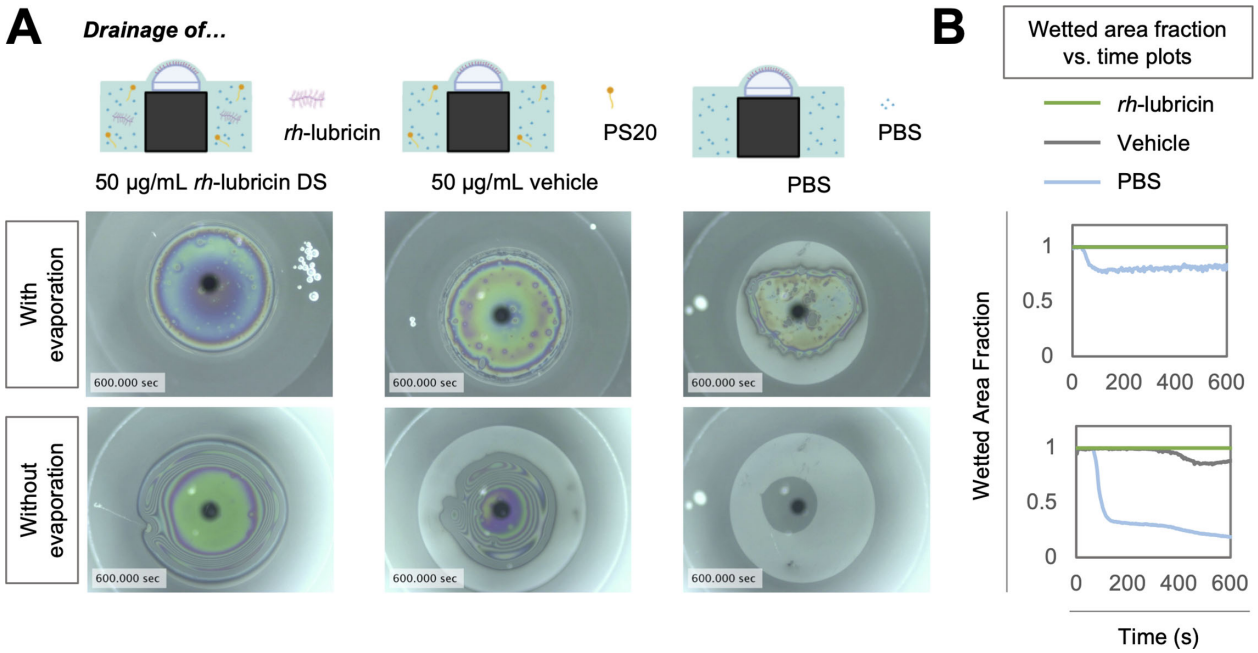

Figure 5. Adsorbed and freely dispersed *rh*-lubricin both play a role in maintaining tear film stability. (**A**) (Top) Representative snapshots following drainage of a high concentration of freely dispersed *rh*-lubricin DS, the equivalent concentration of vehicle, and PBS alone from a glass dome preincubated with a high concentration of *rh*-lubricin DS. Only the PBS condition shows a decrease in area coverage after 10 minutes. Bottom row shows representative snapshots of conditions in (A) when evaporation and thus evaporation-driven Marangoni flow stabilization is suppressed. Only drainage of freely dispersed *rh*-lubricin DS is able to maintain full area coverage after 10 minutes in the absence of evaporation. (**B**) Wetted area fraction versus time plots for conditions shown in (A).

several experiments in which the amount of unstressed *rh*-lubricin adsorbed onto the dome represented the maximum amount possible in any prior experiment (Fig. 5A, Supplementary Movie S5). When comparing the retreat of films containing 50 µg/mL *rh*-lubricin, a vehicle control, and PBS alone, both *rh*-lubricin and the equivalent vehicle control were able to resist evaporative break-up and maintain a fully wetted area over the course of 10 minutes. PBS alone did undergo break-up, but stabilized at a wetted area fraction around 0.8 when the glass surface was coated with adsorbed *rh*-lubricin (Fig. 5B).

Because evaporation was previously identified to have a stabilizing effect in our system,[11] we repeated this set of experiments and suppressed evaporation to further isolate this effect. Without evaporation, oscillatory behavior was no longer present, as expected, and only *rh*-lubricin was able to both resist break-up and maintain the fully wetted area (Fig. 5A, Supplementary Movie S5). The PBS film destabilized most quickly, starting at approximately t = 35 seconds, and reached a final wetted area fraction of 0.2 (Fig. 5B). The vehicle-only film destabilizes approximately t = 300 seconds, but reaches a final wetted area fraction of approximately 0.88. Overall, this set of experiments demonstrated that a high concentration of adsorbed *rh*-lubricin alone was not sufficient to account for the model tear film stability observed in our i-DDrOP experiments.

Discussion

rh-Lubricin is increasingly appreciated for not only its therapeutic potential as a boundary lubricant[6] and anti-inflammatory agent,[18] but also its ability to stabilize model tear films.[11] In this study, we expanded on previous work to condense the rich spatiotemporal data gathered from i-DDrOP experiments into important yet simple-to-use parameters through a robust analysis pipeline. The EBUT and A10 parameters were chosen based on several criteria, namely, reproducibility, ease of calculation, clinical relevance, and the ability to distinguish efficacy. The addition of the mesh top enclosure adds a level of environmental control while still allowing for evaporation, because this factor was shown to be important in the behavior of *rh*-lubricin films. The glass domes used in our system are also reusable, with a pristine glass surface and thus reproducibility ensured by using a highly effective surfactant for cleaning between runs. The A10 parameter

is readily calculated from the analyzed wetted area fraction versus time curve, and the EBUT is analogous to the tear film break-up time commonly used by clinicians to diagnose DED.[19] Because both parameters increase with increasing film stability and *rh*-lubricin concentration, the data can be represented in a familiar dose-dependence curve format, as is commonly used to assess therapeutic efficacy.[20] From such curves, we found that this method is able to identify variations on *rh*-lubricin that are less effective at maintaining tear film stability.

Linear fitting was performed to correct for noise and condense the information into a single value, but we note that the oscillations in wetted area fraction reflect true variations in film coverage. These variations occur in the thinner regions of the film (within the range encapsulating either side of the 50-nm threshold) and are likely owing to the continuous volumetric flux across the glass surface that occurs in the thinner regions of the film.[11] This behavior was most evident at high *rh*-lubricin concentrations, which exhibited a remarkable full recovery of the wetted area after gravity drainage.

Our study on the effect of various industrially relevant stresses revealed that *rh*-lubricin is quite robust in a variety of storage and transport conditions. Elevated temperature stress (4 weeks at 40°C) resulted in the only notable negative shift in efficacy, suggesting that the prevention of aggregation and fragmentation in *rh*-lubricin may be important in therapeutic formulation and storage. Compared with *rh*-lubricin, the vehicle condition showed decreased efficacy and greater variability in its dose response, even when differences in sample size were accounted for. Model tear films consisting of the vehicle were also much less radially symmetric, resulting in uneven coverage of the exposed area. Finally, we note that despite possible differences in *rh*-lubricin length scale owing to aggregation and fragmentation, no detectable differences in film thickness were seen between the variants, which corroborates previous findings that the films are not solely a result of the adsorbed *rh*-lubricin layer on glass.[11]

Our *in vitro* model allows for mechanistic studies regarding adsorption and thin film composition. Previous work has shown that *rh*-lubricin is able to adsorb onto and form a viscous, hydrated layer on hydrophilic glass surfaces,[11] as is the case during our heating step. Other *in vitro* models incorporating corneal and conjunctival epithelial cells also show that both topical treatment using native human lubricin (Seo et al., 2019)[23] and the incubation of cells in solution with *rh*-lubricin[21] resulted in the adherence of lubricin to the epithelial surface. We demonstrated that adsorbed *rh*-lubricin alone was not sufficient to maintain a fully wetted area when *rh*-lubricin was absent from the model tear film. This result suggests that *rh*-lubricin may need to be dispersed freely within the aqueous tear film to achieve the optimal effect on tear film stability, rather than only adhered to the ocular surface.

We note that effective concentrations used in this study are lower than those found to be effective in the clinical trial (150 µg/mL),[9] and that EBUTs observed here are much longer than typical tear film break-up times seen in the clinic. We attribute these differences to a number of factors. For example, our setup offers a more controlled environment than the human eye, where the stability of the tear film is subject to destabilizing influences such as movement, blinking, external contaminants, and so on. We also acknowledge that the gravity vector is typically orthogonal rather than antiparallel to the center of the exposed portion of the eye, which may further destabilize the tear film relative to our system. Furthermore, to incorporate all heating and interferometry-based features, our setup uses a much higher volume than a typical drop of ophthalmic solution (20 mL vs 40 µL)[22] and lacks cellular features, such as surface roughness and the glycocalyx. Nevertheless, the results from our system were able to show differences in efficacy between various forms of *rh*-lubricin and revealed general trends as a function of concentration.

The surfactant PS20 was incorporated into the formulation of *rh*-lubricin to stabilize it in solution. Previous studies have shown that PS20 aids in the adsorption of *rh*-lubricin to hydrophobic surfaces but has a negligible effect on its adsorption to hydrophilic surfaces.[11] Since the air-liquid interface represents another hydrophobic-hydrophilic boundary, PS20 may also help to stabilize *rh*-lubricin at this interface in our system. In this study, we aimed to keep the proportion of PS20 to *rh*-lubricin constant to reflect its role as a stabilizer. If the absolute amount of PS20 in solution were kept constant instead, we anticipate that the incorporation of this increased concentration may further stabilize our model tear films, owing to the behavior we see at high vehicle concentrations (Figs. 4 and 5). In our mechanistic study, we showed that the highest concentration of *rh*-lubricin and vehicle yielded comparable results in solution with evaporation. However, we note that the difference may have been more pronounced at a lower concentration, as was the case with EBUT and A10 (Fig. 4).

The advantages of our system are demonstrated by its ability to obtain reproducible dose-dependent measures of tear film stability in an *in vitro* context, as well as its ability to isolate the effects of the aqueous

component of the model tear film. Our results corroborate those from other *in vitro* model systems of DED that incorporate human corneal and conjunctival cells, which showed that *rh*-lubricin increased tear film break up time and reduced the area of rupture. Although these systems can mimic the blinking motion of the eyelid to show that native lubricin (Seo *et al*., 2019) and *rh*-lubricin[8] can decrease friction during blinking as well as investigate its immunomodulatory functions, our study complements these results by providing a cell-free way to visualize and quantify model tear film thickness, which is challenging in cell-based systems. As in this model, the absence of the outermost lipid layer can be a result of meibomian gland dysfunction, but the i-DDrOP is also compatible with deposition of lipid monolayers at the air–liquid interface.[14] This feature, along with the possibility of functionalized supported lipid bilayers to mimic the mucin layer of the tear film, paves the way toward a more physiologically relevant model of the human tear film that will be useful in future studies.

Acknowledgments

The authors thank Novartis Pharma AG for a research grant and providing *rh*-lubricin for this work. The authors thank N. Rabiah, C. Liu, A. Madl, X. Shi, and L. Engel for discussion. Schematics in Figures 4-1 and 4-5 were created using BioRender.

K.W. Cui is supported by the Stanford EDGE, Bio-X Bowes, and ChEM-H CBI fellowships and National Institutes of Health (NIH) Grant T32GM120007. D.M. is supported by the NIH (National Eye Institute K08EY028176 and a Departmental P30-EY026877 core grant), as well as a core grant and Career Development Award from Research to Prevent Blindness (RPB).

Disclosure: **K.W. Cui**, None; **V.X. Xia**, None; **D. Cirera-Salinas**, Novartis Pharma (E); **D. Myung**, None; **G.G. Fuller**, Novartis Pharma (F)

References

1. Hodges RR, Dartt DA. Tear film mucins: front line defenders of the ocular surface; comparison with airway and gastrointestinal tract mucins. *Exp Eye Res*. 2013;117:62–78.
2. Bansil R, Stanley E, LaMont JT. Mucin biophysics. *Annu Rev Physiol*. 1995;57(1):635–657.
3. Craig JP, Nichols KK, Akpek EKet al. TFOS DEWS II definition and classification report. *Ocular Surface*. 2017;15:276–283.
4. Mantelli F, Argueso P. Functions of ocular surface mucins in health and disease. *Curr Opin Allergy Clin Immunol*. 2008;8(5):477.
5. Holland EJ, Darvish M, Nichols KK, Jones L, Karpecki PM. Efficacy of topical ophthalmic drugs in the treatment of dry eye disease: a systematic literature review. *Ocular Surface*. 2019;17(3):412–423.
6. Schmidt TA, Sullivan DA, Knop E, et al. Transcription, translation, and function of lubricin, a boundary lubricant, at the ocular surface. *JAMA Ophthalmol*. 2013;131(6):766–776.
7. Greene GW, Martin LL, Tabor RF, Michalczyk A, Ackland LM, Horn R. Lubricin: a versatile, biological anti-adhesive with properties comparable to polyethylene glycol. *Biomaterials*. 2015;53:127–136.
8. Liu C, Madl AC, Cirera-Salinas D, et al. Mucin-like glycoproteins modulate interfacial properties of a mimetic ocular epithelial surface. *Adv Sci*. 2021;8(16):2100841.
9. Lambiase A, Sullivan BD, Schmidt TA, et al. A two-week, randomized, double-masked study to evaluate safety and efficacy of lubricin (150 µg/ml) eye drops versus sodium hyaluronate (HA) 0.18% eye drops (vismed) in patients with moderate dry eye disease. *Ocular Surface*. 2017;15(1):77–87.
10. Banquy X, Burdynska J, Lee DW, Matyjaszewski K, Israelachvili J. Bioinspired bottle-brush polymer exhibits low friction and amontons-like behavior. *J Am Chem Soc*. 2014;136(17):6199–6202.
11. Rabiah NI, Sato Y, Kannan A, Kress W, Straube F, Fuller GG. Understanding the adsorption and potential tear film stability properties of recombinant human lubricin and bovine submaxillary mucins in an in vitro tear film model. *Colloids Surf B Biointerface*. 2020;195:111257.
12. Bhamla MS, Fuller GG. *i-ddrop: Interfacial dewetting and drainage optical platform*. Google Patents. 2016, February 23. (US Patent 9,265,413)
13. Bhamla MS, Chai C, Rabiah NI, Frostad JM, Fuller GG. Instability and breakup of model tear films. *Invest Ophthalmol Vis Sci*. 2016;57(3):949–958.
14. Bhamla MS, Nash WL, Elliott S, Fuller GG. Influence of lipid coatings on surface wettability

characteristics of silicone hydrogels. *Langmuir*. 2015;31(13):3820–3828.
15. Rabiah NI, Scales CW, Fuller GG. The influence of protein deposition on contact lens tear film stability. *Colloids Surf B Biointerface*. 2019;180:229–236.
16. Hermans E, Bhamla MS, Kao P, Fuller GG, Vermant J. Lung surfactants and different contributions to thin film stability. *Soft Matter*. 2015;11(41):8048–8057.
17. Suja VC, Verma A, Mossige E, et al. Dewetting characteristics of contact lenses coated with wetting agents. *J Colloid Interface Sci*. 2022;614:24–32.
18. Menon NG, Goyal R, Lema C, et al. Proteoglycan 4 (prg4) expression and function in dry eye associated inflammation. *Exp Eye Res*. 2021;208:108628.
19. Tsubota K. Short tear film breakup time–type dry eye. *Invest Ophthalmol Vis Sci*. 2018;59(14): DES64–DES70.
20. Brown MJ, Sharma P, Mir FA, Bennett PN. *Clinical Pharmacology*. New York: Elsevier; 2019.
21. Madl AC, Liu C, Cirera-Salinas D, Fuller GG, Myung D. A mucin-deficient ocular surface mimetic platform for interrogating drug effects on biolubrication, antiadhesion properties, and barrier functionality. *ACS Appl Mater Interfaces*. 2022;14(16):18016–18030.
22. Kumar S, Karki R, Meena M, Prakash T, Rajeswari T, Goli D. Reduction in drop size of ophthalmic topical drop preparations and the impact of treatment. *J Adv Pharm Technol Res*. 2011;2(3):192–194.
23. Seo J, Byun WY, Alisafaei F, et al. Multiscale reverse engineering of the human ocular surface. *Nat Med*. 2019;25:1310–1318.